Smart Materials in Medicine 5 (2024) 140–152

Contents lists available at ScienceDirect

Smart Materials in Medicine

journal homepage: www.keaipublishing.com/en/journals/smart-materials-in-medicine/

Smartphone-based polydiacetylene colorimetric sensor for point-of-care diagnosis of bacterial infections

Yue Zhou [a,1], Yumeng Xue [a,1], Xubo Lin [a], Menglong Duan [a], Weili Hong [a], Lina Geng [b], Jin Zhou [a,*], Yubo Fan [a,**]

[a] Key Laboratory for Biomechanics and Mechanobiology of Ministry of Education, Beijing Advanced Innovation Center for Biomedical Engineering, School of Biological Science and Medical Engineering, and with the School of Engineering Medicine, Beihang University, Beijing, 100083, China
[b] School of Life Science, Beijing Institute of Technology, 5 South Zhongguancun Street, Haidian District, Beijing, 100081, China

ARTICLE INFO

Keywords:
Bacterial infection
Polydiacetylene (PDA)
Point-of-care (POCT)
Antimicrobial susceptibility testing (AST)
Smartphone-based detection

ABSTRACT

The rapid progress in point-of-care testing (POCT) has become a promising decentralized patient-centered approach for the control of infectious diseases, especially in resource-limited settings. POCT devices should be inexpensive, rapid, simple operation and preferably require no power supply. Here, we developed a simple bacterial sensing platform that can be operated by a smartphone for bacteria identification and antimicrobial susceptibility testing (AST) based on using a polydiacetylene (PDA) arrayed membrane chip. Each PDA array produced a unique color 'fingerprint' pattern for each bacteria based on different modes of action of toxins from bacteria on biomimetic lipid bilayers within PDA-lipid assemblies. We show that the PDA-based device can detect viable cells of bacteria as low as 10^4 CFU/mL within 1.5 h compared with several days of conventional bacterial identification, with the aid of a smartphone app. The device can also be used for an antimicrobial susceptibility test (AST) for at least two broad-spectrum antimicrobials within 4 h and provide identification of antimicrobial susceptibility and resistance, enabling the selection of appropriate therapies. This PDA-based sensing platform provides an alternative way for bacterial detection and could be used as a portable and inexpensive POCT device for the rapid detection of bacterial infection in limited-resource settings.

1. Introduction

The monitoring and diagnosis of bacterial infections are crucial for clinical management. Especially, controlling antimicrobial-resistant infections is a unique challenge worldwide. Improving bacterial infection diagnosis is crucial for guiding antimicrobial therapy, but it remains challenging due to unspecific clinical presentations. Distinguishing between pathogenic and non-pathogenic bacteria and closely related subspecies poses a key issue. Conventional culture methods cause delays in accurate antimicrobial administration, fostering antimicrobial resistance. In resource-limited settings, the shortage of professionals and high-tech instruments raises the risk of medication misuse. Clinical decisions often rely on symptoms, contributing to antimicrobial resistance. On the other hand, the high cost and lack of skilled personnel hinder the popularization and application of POCT (point-of-care testing) devices [1–3]. Taking UTI (Urinary-Tract-Infections) for instance, the administration of a community-acquired UTI is generally based on empirical antimicrobial therapy [4,5]. Many studies have reported that symptoms based UTI diagnosis places a large number of patients at a high risk of prescription of unnecessary antimicrobials [6–9]. Furthermore, UTI is recognized as one of the most common causes of infection. Patients with long-term bladder catheterization are at a high risk of UTI, including elderly people, disabled patients, or patients with spinal cord injuries. It is not surprising that the frequency of indwelling urinary catheters (IUC) can cause most cases of nosocomial infections caused by catheter-associated urinary tract infections (CAUTIs). Several types of POCT devices for the detection of bacterial infections have been developed, but not all can be applied in such situations [1,10–14]. Most of them require complex manufacturing procedures as additional equipment for detection. Developing affordable and practical POCT devices is crucial for early infection screening in resource-limited settings. These devices must offer rapid detection and easy operation to alert patients

* Corresponding author.
** Corresponding author.
E-mail addresses: jinzhou@buaa.edu.cn (J. Zhou), yubofan@buaa.edu.cn (Y. Fan).
[1] Y.Z.and Y.X., contributed equally to this work.

https://doi.org/10.1016/j.smaim.2023.10.002
Received 4 August 2023; Received in revised form 11 October 2023; Accepted 12 October 2023
Available online 25 October 2023

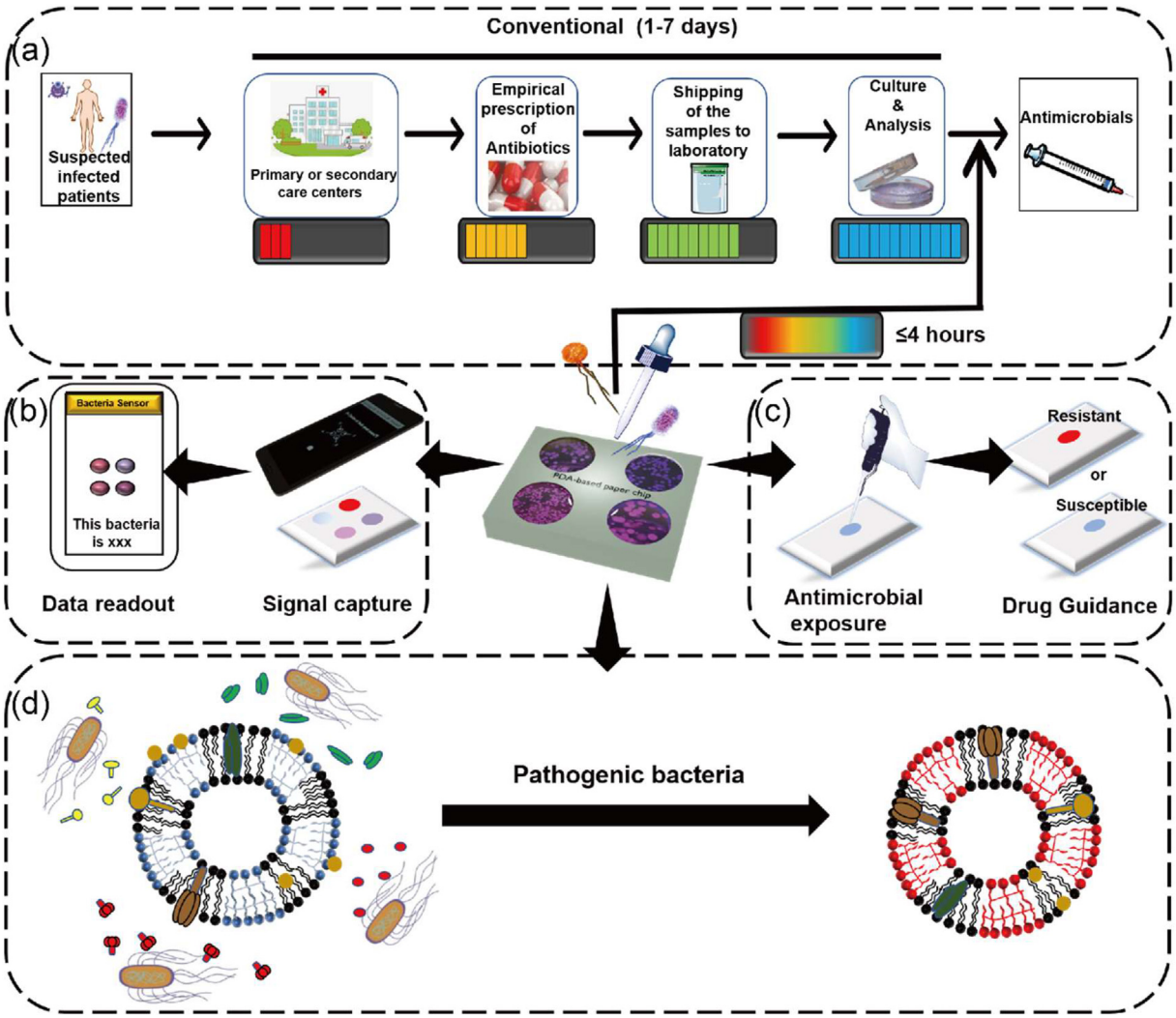

Fig. 1. The PDA-based sensor platform for detecting bacteria and drug susceptibility at resource-limited settings. (a) Conventional methods for diagnostics of bacterial infection (b) Smartphone-assisted bacteria sensing procedure including unknown samples dropped onto the membrane chip, signal capture by built-in camera of the smartphone, and data analyzing & results display by a 'Bacteria Sensor' app. (c) Detection of bacterial susceptibility to antimicrobials for the identified bacteria, providing AST results to avoid antibiotic resistance. (d) Mechanism of colorimetric transition of PDA-lipid assemblies (liposomes) by bacterial toxins due to the existence of polydiacetylene backbone in bilayer assemblies.

and caregivers to potential infections. The diagnostic approach should prioritize speed, accuracy, and sensitivity for early screening of pathogenic bacteria, along with identifying antimicrobial susceptibility and resistance. An ideal device should be suitable for both limited-resource settings and well-developed nations, allowing rapid testing with low costs and no need for specialized technical skills.

Diagnostic strategy-based colorimetric assay has shown great advantages in POCT as such assay can be regarded as one kind of portable sensor system without requirements of complex instrumentations or technical skills [15–25]. In addition, the results can be recognized by direct visualization through colorimetric transitions. Polydiacetylene (PDA), an amphiphilic conjugated polymer, has drawn much attention as a chromatic sensing material due to its unique chromatic transition from blue to red color perturbed by external stimuli such as temperature, pH, and biomolecules, etc. Likewise, lipid vesicles (liposomes) with incorporated PDA can present chromatic colorimetric transition. Generally, phospholipids and diacetylene (DA) monomers self-assemble on various substrates to form highly assembled aggregates. After UV irradiation, the literally stacked DA monomers form extended π-conjugated backbones, rendering the assemblies to exhibit blue color. So far, sensors based on PDA have been widely researched for the detection of biological and chemical molecules either based on aqueous-phase or solid-phase sensors [24,26–44]. Aqueous-phase sensors, basically PDA liposome solution, have shown internal aggregation during long-term storage because of the relative instability of PDA solution, whereas solid-phase PDA sensors (immobilization of PDA assemblies on various substrates) serve as more suitable POCT sensors, generating inexpensive, flexible and lightweight PDA-based sensor systems with customized designs or patterns. In addition, PDA biosensors to detect various biomolecules, especially bacteria are mainly based on PDA functionalization. Information on ligands or specific receptors of each opportunistic pathogen is required, as well as the laborious synthesis process of ligands conjugated to the lipids, thereby limiting the development of bacterial diagnosis. Our previous work has demonstrated that lipid compositions and especially cholesterol contents within PDA-lipid bilayers play an important role in the susceptibility of the colorimetric response of PDA-lipid liposomes to bacterial toxins [45]. Based on the theory of previous investigations, we mainly focus on immobilizing PDA-lipid assemblies onto a membrane substrate to build a solid-phase PDA sensing platform, making them suitable as POCT devices.

With the increase in the number of smartphone users worldwide, the ability of these devices to data processing is also growing. With the

emergence of smartphones and the needed networks, the costs of global data acquisition and transmission are rapidly reducing. In 2016, global smartphone users reached 51 % [46] and it has been reported that by 2020 in sub-Saharan Africa the number of smartphone users has reached 55 % [46]. Meanwhile, users can use smartphone application software (apps) to create customized mobile applications without knowledge of computer programming. This powerful pocket computer has built-in sensors and a wireless connection, which provides a new opportunity for health systems to obtain data capturing and the subsequent results. With the reduced affordability barriers by the low-cost spreading utility of smartphones, the adoption of smartphones and their related technologies in both resource-rich and resource-limited settings is continually growing. Such technologies will offer capabilities of sensing and processing comparable to more costly "high-end" technologies. In the context of designing new strategies for bacterial diagnosis, we assumed smartphones can serve as high-performance built-in cameras and mobile applications for image analysis, preserving the abilities of bacterial identification by replacing expensive and heavy instrumentation.

PDAs with different lipid compositions can undergo chromatic color transition with the treatment of various bacterial species [45,47–52]. However, determining the identity of one specific bacteria based on the colorimetric transition of one single PDA-lipid assembly is extremely challenging. The previous work has demonstrated that aqueous-based PDA-lipid assemblies (liposomes) composed of different contents of cholesterol can achieve fingerprint identification of each bacterial strain through different color patterns in response to various bacterial strains [45]. The strategy was mainly based on the interaction of toxins produced by bacteria and lipid bilayers, causing PDA backbone distortion and subsequent colorimetric transition. Here, we adopted the "combinatorial" strategy and immobilized the PDA-lipid arrays on a paper-like (PVDF membrane) substrate to simplify and improve the flexibility for bacteria sensing. The PDA-based sensor was integrated with a conventional smartphone system for fast data processing. The study uses a library of PDA-lipid assemblies, displaying different color responses to various bacterial strains. Considering the above factors, the proposed biosensing platform integrated with a smartphone app readout based on PDA arrayed paper-like chip has been engineered for bacteria identification and subsequent antimicrobial susceptibility testing. The results demonstrated that the PDA-arrayed chip can inform the presence of viable cells and distinguish at least four bacterial species within 2 h compared with several days of conventional bacterial identification (Fig. 1a). With the aid of our pre-programmed smartphone "app", the relatively low concentration of bacterial cells can be identified. In clinical scenarios, this will help patients identify appropriate antibiotics/antimicrobials among those who have suspected symptoms. Furthermore, we performed a simplified AST (antimicrobial susceptibility test) to allow the completion of the whole testing process within approximately 4 h including identification of bacterial cells (Fig. 1b). The proposed biosensing platform may offer a feasible alternative to traditional ASTs, especially in resource-limited settings.

2. Materials and Methods

2.1. Design and working principles of the smartphone-based biosensor

The smartphone-based PDA membrane biosensor is a flexible device integrating a PDA arrayed chip with a smartphone app with data built-in. The design process incorporates three parts: first, PDA-lipid complexes with four different contents of cholesterol (Table S1) were immobilized onto a paper-like substrate (PVDF membrane) and the PDA arrayed chip comprising four arrayed spots were treated with 5 different bacterial strains, individually. In response to the respective bacterial strain, each PDA array generated a unique color pattern. Second, image data were collected including RGB values corresponding to each specific bacterial strain by analyzing the colorimetric response of each PDA array; then, the bacterial diagnosis app was developed by analyzing the database of R intensity from the interaction of PDA arrays and pathogenic bacteria. Third, an unknown bacterial sample was dripped on the PDA arrayed paper-like chip, and the image was captured by the built-in camera of the smartphone, and the image processed by the app finally provided the user with fast and direct result readout (Fig. 1c and d). The principle of the sensor design was based on the different response sensitivities of PDA-lipid assemblies to various pathogenic bacteria by varying concentrations of cholesterol [45]. The PDA-lipid assemblies can efficiently distinguish different bacterial strains, by varying cholesterol compositions. The mechanism behind this was based on different modes of action of bacterial toxins on membrane-like lipid bilayers. PDA-lipid assemblies, acting as membrane-like lipid bilayers, occurred in different chromatic transitions, triggered by different bacteria. Therefore, each PDA-lipid array exhibited unique chromatic patterns for each bacterial strain. The previous work has systematically investigated the mechanism of chromatic transition perturbed by bacteria based on liquid-phased PDA liposomes. To render the sensing platform more flexible and applicable in resource-limited regions, solid-phase PDA biosensor based on PDA-lipid arrays was utilized in the present work, each array composed of different molar ratio of cholesterol/phosphatidylcholine in PDA assemblies (Table S1).

2.2. Synthesis of PDA-lipid complexes

DSPC (1,2-distearoyl-*sn*-glycero-3-phosphocholine18:0) was obtained from Avanti Polar Lipids, US. Cholesterol (Chol) and 10, 12-pentacosadiynoic acid (PCDA) were purchased from Sigma-Aldrich. All materials used in the study were not purified further.

PDA liposomes, the liquid-based PDA-lipid complexes, were synthesized through the thin film evaporation method, which has been detailed previously [45]. Briefly, PDA-lipid complexes comprising fixed contents of PCDA and different molar concentrations of cholesterol and DSPC were dissolved in chloroform, forming the lipid mixture. The lipid mixture was dried under nitrogen gas to form a thin lipid film around a glass bottle, followed by Tris buffer addition. The resultant lipid solution was sonicated for 30 min to form self-assembled lipid vesicles. The resultant vesicle solution was annealed at 4 °C for 16 h before conducting UV-polymerization (254 nm).

2.3. Formation of solid-phase PDA arrayed chips

2 mM of PCDA, CHO, and DSPC with different molar ratios (Table S1) were mixed in 2 mL of chloroform. PVDF membranes were cut into 3 cm × 3 cm squares by scissors. 100 mL of four different compositions of lipid mixture was pipetted on the surface of the PVDF membrane and dried under nitrogen to form a solid-based PDA arrayed chip. The PDA arrayed chip was cooled at 4 °C for 16 h before UV irradiation for 1 min, which changed the PDA array from colorless to blue. The PDA arrayed membrane chip was characterized by FT-IR and was stored away from light at 4 °C for further use.

2.4. Components and classification of PDA arrays

In this study, each PDA arrayed membrane chip is capable of identifying one bacterial species by a unique chromatic pattern (Fig. 1b). The PDA-arrayed chip comprised four PDA-lipid complexes to form a PDA array for bacterial detection. The complex primarily comprised fixed content of PCDA (40 mol%), with various DSPC and cholesterol (CHO) concentrations, which are shown in Table S1. In the present study, we selected four PDA-lipid complexes of Ves 1 (40 % PCDA, 60 % DSPC, 0 % CHO), Ves 2 (40 % PCDA, 40 % DSPC, 20 % CHO), Ves 3 (40 % PCDA, 20 % DSPC, 40 % CHO), and Ves 4 (40 % PCDA, 10 % DSPC, 50 % CHO) for the subsequent study.

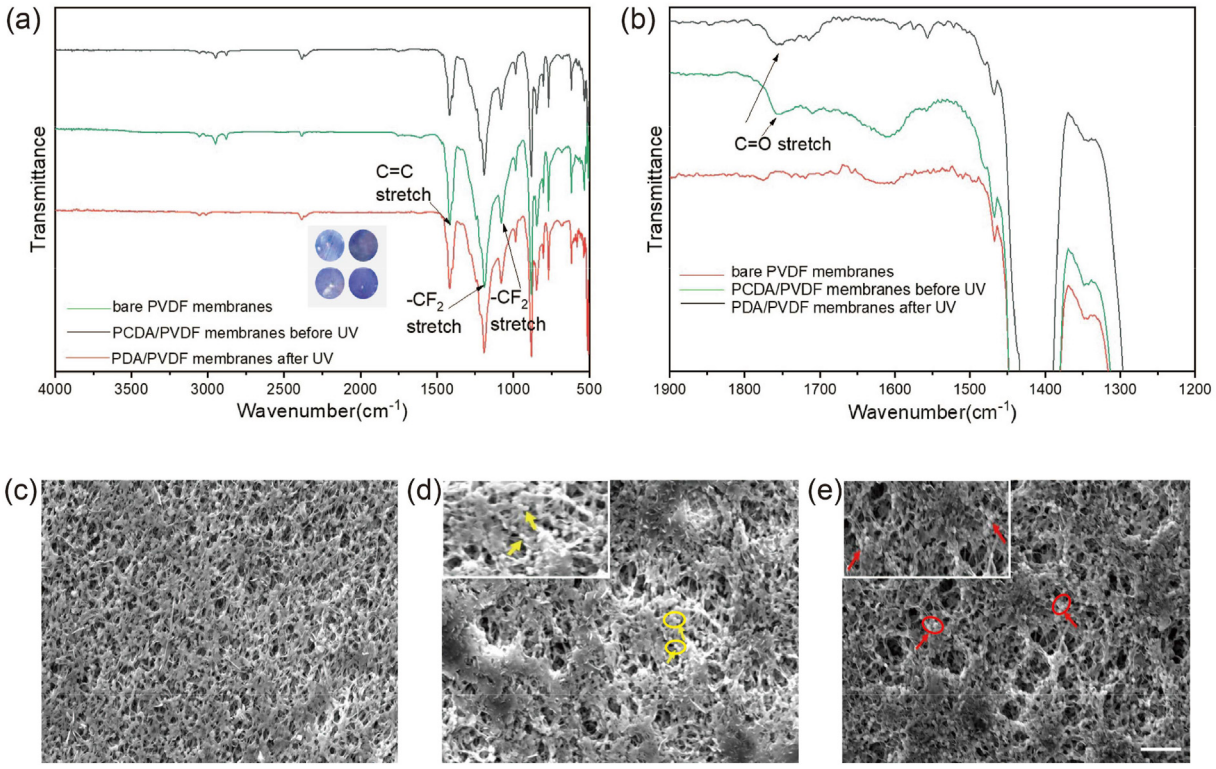

Fig. 2. FT-IR and SEM characterization of immobilized PDA-lipid complexes on PVDF membranes. (a) (b) FT-IR characterization of immobilized PDA-lipid complexes. Fig. 2b is an enlarged version of Fig. 2a. The insert image shows four blue PDA-lipid spots on a PVDF membrane after UV polymerization. (c) (d) (e) SEM images of pure PVDF membrane (c) PDA-PVDF membrane (d) and PDA-PVDF after treatment with *S. aureus*. Yellow arrows (d) are dedicated PDA liposomes on PVDF membranes, while red arrows (e) dedicating bacteria aggregated on the surface of the PDA-PVDF membrane. Scale bar: 10 μm.

2.5. Bacterial culture

E. coli (ATCC 25922), *S. pneumoniae* (ATCC 49619), *E. faecalis* (ATCC 29212), *S. aureus* (CMCC 26003), *P. aeruginosa* (CMCC 10104), *K. pneumoniae* (CMCC 46117) were obtained from ATCC or CMCC (National Center for Medical Culture Collections). The six bacterial strains were considered pathogenic bacteria and can secret a series of toxins that can lyse lipid membranes. In the experiment, growth medium including Luria-Bertani Broth (LB), Tryptic Soy Broth (TSB), and BHI (Brain Heart Infusion Broth) were used for bacteria culture. LB was used for *P. aeruginosa*, *E. coli*, and *E. faecalis*; TSB for *S. aureus*; BHI for *K. pneumoniae*. Briefly, 100 mL of growth medium with bacteria were cultured in an incubator overnight (150 rpm, 37 °C). 100 μL of overnight bacterial culture were incubated with 10 mL fresh growth medium for another 4 h, rendering the bacteria in the exponential growth phase. Bacteria are believed to produce more virulent toxins/enzymes at this stage, and bacteria at this stage are called sub-cultured bacteria. The sub-cultured bacteria were used in the subsequent study unless otherwise specified.

2.6. Dose response of chromatic properties of PDA-PVDF membrane

PDA-lipid complexes comprising 25 mol% cholesterol as a representative PDA sensor in the study, *S. aureus,* and *P. aeruginosa* as model bacteria were utilized in the assay. The sub-cultured *S. aureus* and *P. aeruginosa* were centrifuged at 10,000 rpm and re-suspended in physiological saline buffer, respectively. Each bacterial strain solution was diluted with concentrations of 10^3, 10^4, 10^5, 10^6, and 10^7 CFU/mL according to the standard curve of optical density at 600 nm against each bacterial colony forming unit per mL. The results were detailed in supplementary data (Figure S2). 10 μL of each diluted bacteria solution was added onto the PDA-lipid complex spot on the PVDF membrane and incubated for 1 h at 24 °C. The chromatic color change of each PDA spot was analyzed using digital images (captured by a built-in smartphone camera) before and after exposure to different concentrations of bacteria for a total period of 1 h. A smartphone built-in camera was used to capture the images of the PDA-lipid spot, and the RGB values were evaluated via Image J software over 30 × 30 pixels (~65 % of total area). The results were normalized relative to the controls. All tests were carried out in triplicate.

2.7. Quantitative analysis of PDA-arrayed membrane chip

To demonstrate the colorimetric response of the PDA array to each bacterial strain, 10 μL of the bacterial solution with a concentration of 10^6 CFU/mL L was added to four arrayed spots of PDAs. The time evolution of the colorimetric transition in the PDA arrayed membrane chip was recorded by taking photographs after 1 h. Colorimetric transitions were hardly observed significantly within 1 h in all cases of 5 bacterial strains. The 1-h snapshots were chosen to analyze the colorimetric response of the PDA-arrayed chip. To construct an R database for the subsequent app development, R values of arrayed PDA spots treated by each bacterial strain were analyzed by ImageJ software (≥20 tests). To measure the R intensity, the interested regions were analyzed in the image. For each region of interest, we use the circular Hough transform to locate the circular region. The smartphone's built-in camera was used to capture the pixels of the circular region of interest. R values were normalized by using calibration factors and shown in Fig. 4b. The calibration factors were obtained from the center spot (blue circle) of each detection screen with a background among four PDA arrayed spots (Fig. 6b). For example, when the RGB values of the calibration spot with the background were analyzed as (178, 176,154), the calibration factors were calculated as (12, 14, 36), based on the standard RGB values of (190, 190, 190). R values used in the study were all normalized by using

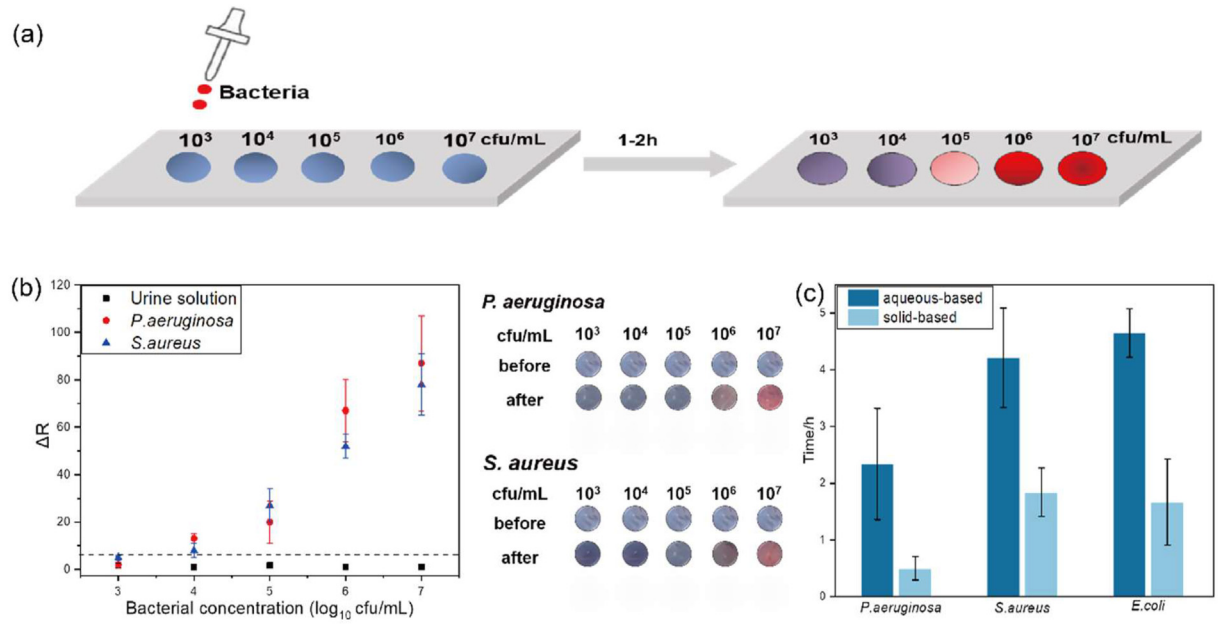

Fig. 3. Chromatic response of immobilized representative PDA-lipid complexes composed of 25 % cholesterol induced by *P. aeruginosa* and *S. aureus*. (a) Schematic illustration of dose-response of PDA membrane chip by treatment of bacterial strains. (b) Quantification of colorimetric dose-response of immobilized PDA-lipid complexes upon treatment of *P. aeruginosa* and *S. aureus*. The insert image shows increased Redness induced by an increased concentration of inoculated bacteria. (c) Response time of immobilized PDA-lipid complex compared to aqueous phase-based PDA liposomal systems. All data are shown as mean ± s.d. Based on three paralleled experiments.

an identical calibration process. All measurements were tested at 24 °C.

2.8. Molecular dynamics (MD) simulations

In this work, all-atom MD simulations were performed using GROMACS software [53] (version 2019.03) and CHARMM36 force field [54,55]. CHARMM36-compatible parameters for polydiacetylene (PDA) were adapted from previous research [56]. Four symmetric membrane systems, 18 PDA molecules, 180 lipids (a. DSPC: Chol = 4:1, b. DSPC: Chol = 1:1, c. SPC: Chol = 4:1, d. SPC: Chol = 1:1), 13,305 TIP3 as well as 0.15 M NaCl were studied. The Lennard-Jones potential was smoothly shifted to zero between 1.0 and 1.2 nm, with a cutoff of 1.2 nm to reduce cutoff noise. Particle mesh Ewald [57–59] electrostatics with a real-space cutoff of 1.2 nm was used. The systems were coupled to Nose-Hoover heat baths at T = 298 K (coupling constant τ = 1 ps) and 1 bar pressure using a semi-isotropic Parrinello-Rahman pressure coupling scheme [60] with a coupling constant $\tau = 5$ ps and compressibility of 4.5×10^{-5} bar^{-1}. Bonds with H-atoms were constrained with the LINCS algorithm [61]. The non-bonded interaction neighbor list was updated every 20 steps with a cutoff of 1.2 nm. 100ns all-atom MD simulation with the time step of 2fs and trajectory-saving frequency of 10ps was performed for each system. System snapshots were generated by VMD [62].

2.9. AST assay

P. aeruginosa and *S. aureus* were used as representative bacterial strains for evaluating the AST performance. Minimum inhibitory concentrations to kill 50 % (MIC_{50}) and 90 % (MIC_{90}) of the bacterial populations of gentamicin sulfate (Sigma Aldrich) and ciprofloxacin (Sigma Aldrich) against the two strains were individually evaluated before AST assay. The MIC results are listed in Table S2. The antimicrobial solutions were prepared according to the manufacturer's instructions with serial dilutions in phosphate-buffered solution. Overnight-cultured *P. aeruginosa* or *S. aureus* (~10^7 CFU/mL) was inoculated in different concentrations of gentamicin sulfate and ciprofloxacin, respectively, for a total of 30 min. The mixture was then dripped onto the PDA paper chip for red intensity identification after bacterial confirmation. All experiments were repeated three times at a given set of conditions.

3. Results and discussion

3.1. Formation and characterization of PDA-immobilized PVDF substrate

PDA-lipid complexes were immobilized on a PVDF membrane and the successful immobilization was confirmed by FT-IR and direct visualization of chromatic change by UV irradiation (Fig. 2a the insert image). PDA membrane chips capable of detecting various bacteria were formed and the process of formation was described in the Materials and Methods. Self-assembled monolayers of a mixture of PCDA, lipid (DSPC), and cholesterol were added onto a PVDF membrane. Various parameters were attempted to optimize the immobilization conditions [25,32,38,63]. Here, the PVDF membrane is composed of lipid and cholesterol parts responsible for the docking and insertion of bacterial toxins, whereas the PDA part serves as a module for visual signal generation. A chromatic transition from colorless to blue was visually confirmed by UV irradiation, suggesting that PCDA was successfully photopolymerized and immobilized on the PVDF membrane. Here, the PVDF membrane served as the support to form a self-assembled PDA (Fig. 2a, the insert image). The chemical compositions of the PVDF membrane were measured by FT-IR, and the PVDF membrane displayed characteristic absorption bands at both ~1190 cm^{-1} and~1410 cm^{-1}, associated with $-CF_2$ stretching and C═C stretching, respectively (Fig. 2a and b). After PDA was immobilized on the PVDF membrane, the weak absorption bands of C═O stretching vibrations correspond to carboxylic acids in both PCDA and PDA present at 1750 cm^{-1} (Fig. 2b). In addition, the microscopic structure of the PDA-PVDF membrane surface was observed by SEM imaging (Fig. 2c–e). The porous structure of the membrane surface showed similar before and after UV irradiation, compared to those of bare PVDF membranes.

3.2. Performance of PDA membrane chip

The present assay investigates whether the PDA membrane chip was an ideal POCT device for bacterial detection. Most PDA-based sensors

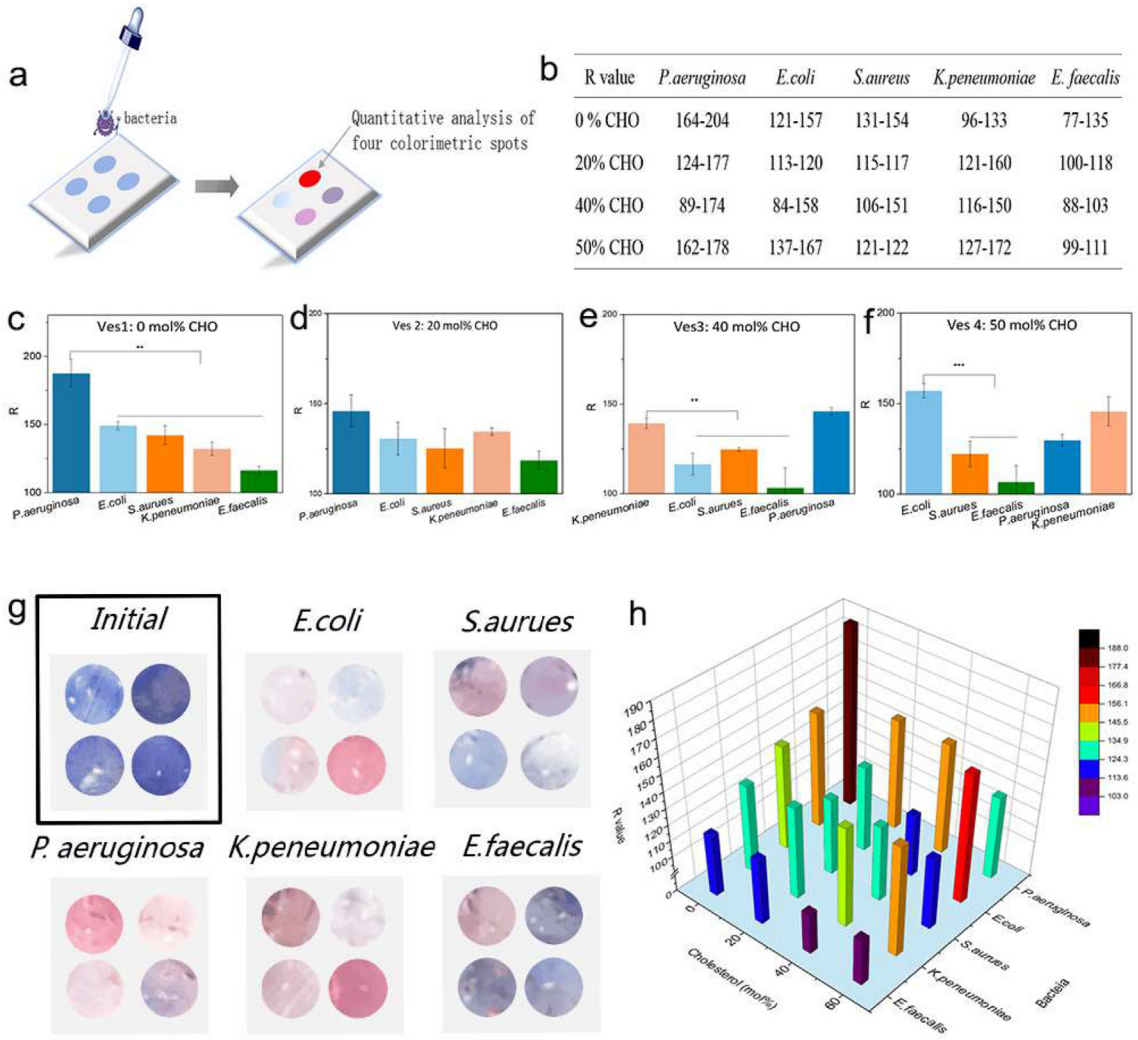

Fig. 4. Quantitative analysis of PDA-based sensing platform. (a) Schematic illustration for analyzing the sensing system. (b) Database of the normalized R values for bacterial responses of PDA-lipid complex with various cholesterol contents. (c) (d) (e) (f) R values of PDA-lipid complex comprising various contents of cholesterol (Ves 1-Ves 4) after treatment with the five bacterial strains. (g) The corresponding color patterns when PDA spots (Ves1-Ves 4) were exposed to each bacterial strain. (h) The recorded R values of the four PDAs are depicted in (c)–(f). The quantitative analysis of R values of the colorimetric pattern of each bacterial strain was based on colorimetric transition images of (g).

have relied on the functionalization of a carboxylic acid group for the detection of specific microorganisms. The strategy, by simply utilizing more conventional lipid components instead of ligand conjugation, broadly increased its practical application in the field of bacterial diagnosis without any further ligand selection. Here, we attempted to develop PDA membrane chips that can detect bacterial toxins secreted by pathogenic bacteria based on the actions of bacterial toxins on lipid membranes. The ability of the PDA membrane chip to detect pathogenic bacteria at various concentrations was first evaluated to confirm the detection limit. Aqueous-based PDA sensors were evaluated as a comparison (Figure S1). PDA-lipid complexes comprising 25 % cholesterol as representative PDA sensors, *S. aureus,* and *P. aeruginosa* as model bacteria were utilized in the study. 10 μL of the two bacterial strains were individually dropped on the PDA membrane chip, as indicated in Fig. 3a. The colorimetric transitions that occurred on the PDA membrane chip were visually monitored and scanned, after 1 h incubation at room temperature (Fig. 3a). The quantification of redness intensity treated with various concentrations of the bacterial strains was evaluated. The efficacy of the experiment was set within a time frame of 1 h as the prototype sensor can be better applied to the timely detection of POCT.

As shown in Fig. 3b, the blue PDA-lipid spot gradually turned to red after bacteria inoculation and the intensity of red color tended to increase, exhibiting a dose-response manner as each bacterial concentration increased. Here, to investigate the effects of PDA membrane chip on UTI (urinary tract infection) detection. Artificial urine, as a control, was used in the study. The results showed that the PDA spot maintained blue with the treatment of the urine, regardless of its increased concentration (Fig. 3b), whereas aqueous-based liposomes were shown less sensitivity induced by *P. aeruginosa* and *S. aureus* respectively within 1 h incubation (Figure S1). In Fig. 3b, samples with bacterial concentrations of 10^5–10^7 CFU/mL were confirmed to be the effective ones with the range of detection in solid-phase PDA chips. At the concentration below 10^5 CFU/mL, the overall red intensity was definitely changed confirmed by the spectrophotometer, although it was hardly to be distinguished by visible observation. The intensity of redness of the PDA-membrane chip at 10^4 CFU/mL was measured to be 4 folds more redness than the concentration of 10^3 CFU/mL (Fig. 3b). Accordingly, the measurement of red intensity needed to be detected by more professional equipment and software. In addition, the R values in both *S. aureus* and *P. aeruginosa* changed slightly in accordance with their corresponding images, and thus a semi-quantitative estimation of bacterial concentration can be obtained by visual comparison to the color chart (Fig. 3b, insert images).

The PDA membrane chip showed more sensitive detection ability, compared with aqueous-based PDA sensors with a minimum detection concentration of 10^6 CFU/mL (Figure S1). Additionally, in order to increase the visual color of redness and to decrease detection time, the PDA membrane chip could be incubated at 40 °C for 10 min before bacteria treatment. This was based on the previous assumption that external relatively high temperatures (36 °C–50 °C) may weaken the stability of PDA conjugated backbone without affecting thermochromic colorimetric transitions of PDA, and thus this would increase redness contrast and reduce detection time by subsequent bacteria addition [64–67]. From Fig. 3, *P. aeruginosa* showed slight sensitivity to the PDA spot, compared with *S. aureus*, due to different modes of action of toxins secreted by each bacteria on biomimetic lipid bilayers within PDA-lipid assemblies.

Time-to-Detection (TTD), defined as the time point when R values significantly exceeded the artificial urine solution, of both solid and aqueous based PDA sensors were evaluated (Fig. 3c). Solid-based PDAs showed smaller DTT, compared to PDA liposome solution [45], indicating higher sensitivity and relatively rapid response time to bacteria.

Collectively, although the PDA membrane chip enables color visualization at relatively high concentrations (10^5 ~10^7 CFU/mL), the visualization of small differences in colorimetric transitions at low concentrations by the naked eye was exceptionally challenging. Accordingly, a smartphone-based detection platform was necessary for fast and accurate detection. Furthermore, the linear relationship between redness intensities (R) and bacterial concentrations may provide a theoretical basis for the subsequent development of quantitative detection of infectious concentrations of definitive bacterial species and drug susceptibility.

3.3. Analysis of color-fingerprinting database based on PDA membrane chip treated with various bacterial species

The previous study has shown that PDA-lipid arrays with different embedded lipid components, especially cholesterol, were able to distinguish various bacterial species, based on different modes of action of bacterial toxins on cholesterol embedded bilayers. In addition, cholesterol, present specifically in eukaryotic cell membranes and recognized as a target molecule for some bacterial toxins, is involved in the recognition and interaction of pore-forming toxins produced by some bacteria such as pneumolysin from K. pneumonia, thereby the presence and amount of cholesterol in the cell membrane can affect the susceptibility of the cell membrane to certain bacterial toxins, which has been experimentally confirmed by the previous findings [45]. The secreted biomolecules/toxins can exhibit different surface charge, hydrophilicity, chemical structures, and other properties, and the interaction between biological molecules with phospholipid bilayer mainly cholesterol can influence the nearby alternating triple-bond/double-bond backbone structure of PDA, leading to different colorimetric response (CR%). Here, to demonstrate the feasibility of a PDA membrane chip, an information database of colorimetric transitions (RGB) of four different PDA-lipid arrays upon perturbation by five chosen bacterial strains was generated for the subsequent development of image-analysis-based smartphone app (Fig. 4a). Four strains of bacteria that may cause infectious disease in hospitals were used as model bacteria to explore the sensitivity to PDA arrayed membrane chip. *E. faecalis* was used as a control model as the strain did not secrete any enzymatic toxins when interacted with eukaryotic cell membranes thereby causing no/little colorimetric transition of PDA-lipid complexes, confirmed by the previous study [45]. The influence of cholesterol concentration on the sensitivity of the PDA-lipid complex to the five bacteria was imaged and explored by quantifying the red intensity (R) of RBG of each PDA array. Four spots of PDA-lipid complexes comprising different concentrations of cholesterol (Ves 1, Ves 2, Ves 3, and Ves 4) were immobilized on the PVDF membrane to form a PDA paper-like chip for each bacterial identification (Fig. 4a). Initially, the immobilized PCDA-lipid array was invisible and UV irradiation (254 nm) was used to polymerize PCDA, leading to the production of PDAs and the corresponding appearance of the blue color of the four spots. Upon individual treatment of each bacterial strain, the chromatic change of the four arrayed spots occurred, from blue to red, generating a unique color pattern for each bacterial strain. The color pattern was visibly differentiated by the naked eye despite their similar polarities (Fig. 4g) and the quantification of PDA arrayed membrane chip to bacterial strains was also shown in Fig. 4c–f.

From Fig. 4c–f, for example, both *P. aeruginosa* and *S. aureus* promoted distinguishable colorimetric fingerprinting patterns on the PDA membrane chip (Fig. 4h). The color transition of Ves 1 (0 % CHO) caused by *P. aeruginosa* was more noticeable than that promoted by *S. aureus*. Phospholipase secreted by *P. aeruginosa* here is involved in the main membrane damage activity and hydrolyzes phosphatidylcholine of PDA-lipid complexes. DSPC in the PDA-lipid complexes provided hydrolyzing sites for toxins from *P. aeruginosa* regardless of the rigidity of lipid bilayers, leading to higher levels of PDA structure conformation and subsequent more intense red color change. α-Hemolysin from *S. aureus* caused a less intense red color, due to its participation in pore formation mediated membrane damage independent of cholesterol contents. Ves 1 comprising more phosphatidylcholine provided more binding sites for pore formation and thus *S. aureus* showed relatively high red intensity to Ves 1, compared with Ves 5. The relationship between the extent of colorimetric transitions and lipid compositions within PDA-lipid bilayers has been detailed in the previous study [45]. Our goal was to develop a solid-phase-based PDA sensor, rendering it more suitable for POCT application in multiple scenarios.

The R values were extracted by using ImageJ software. Higher R values corresponded to more intense red colors, meaning that PDA-lipid complexes were more sensitive to a bacterial strain. The PDA-lipid complex containing 0 % cholesterol showed relatively high sensitivity to α-hemolysin from *S. aureus* and *E. coli*, compared to pneumolysin from *K. pneumonia*, which is recognized as cholesterol-dependent pore-forming toxins (Fig. 4c). *P. aeruginosa* showed the highest sensitivity among the other four bacterial strains regardless of cholesterol contents, due to hydrolysis of phosphatidylcholine (DSPC) independent of cholesterol concentration (Figure *c*–e). In addition, DSPC with the highest concentration (60 %, Ves 1) provided more hydrolysis sites by toxins from *P. aeruginosa*, resulting in the highest level of conformation of PDA backbones (Fig. 4c).

K. pneumoniae showed gradually increased sensitivity with the increase of cholesterol concentration and showed the highest R value in Ves 4 (Fig. 4c–f). The mechanism induced by *K. pneumoniae* may account for the cholesterol-dependent pore formation and thereby a large amount of cholesterol in the PDA-lipid complex provided more binding sites for *K. pneumonia*, resulting in the highest intensity of redness. This was also reflected by the strong red color on the PDA membrane chip (Fig. 4g).

E. coli generated a low R value (<150) in Ves 1, 2, and 3, which was also reflected by the less intense of red color on the image of the PDA membrane chip (Fig. 4c–e, g). The low concentration of cholesterol may account for the rigidity of the lipid bilayer, resulting in a decrease of liposome reactivity, hindering the effective binding or activation bilayer of the toxin on the lipid bilayers. In contrast, high concentrations of cholesterol showed the most sensitivity to *E. coli* with an R value of 157 (Fig. 4f).

S. aureus showed relatively stable red values in Ves 1–4, indicating the sensitivity of *S. aureus* may not be closely related to cholesterol concentration (Fig. 4c–f). This was somewhat contrary to the previous results (the sensitivity of *S. aureus* to PDA can be enhanced by an increase in cholesterol concentration) based on an aqueous PDA sensor [45]. The solid-phase-based PDA sensors increased the contact possibility between toxins from *S. aureus* and lipid bilayers, resulting in the relevant sensitivity to each PDA-lipid complex, although the aqueous-based sensors showed little/no response to *S. aureus* at the low concentration of cholesterol. The relevant mechanism is described by MD simulation in the following study.

Collectively, the R values of each PDA-lipid array corresponding to

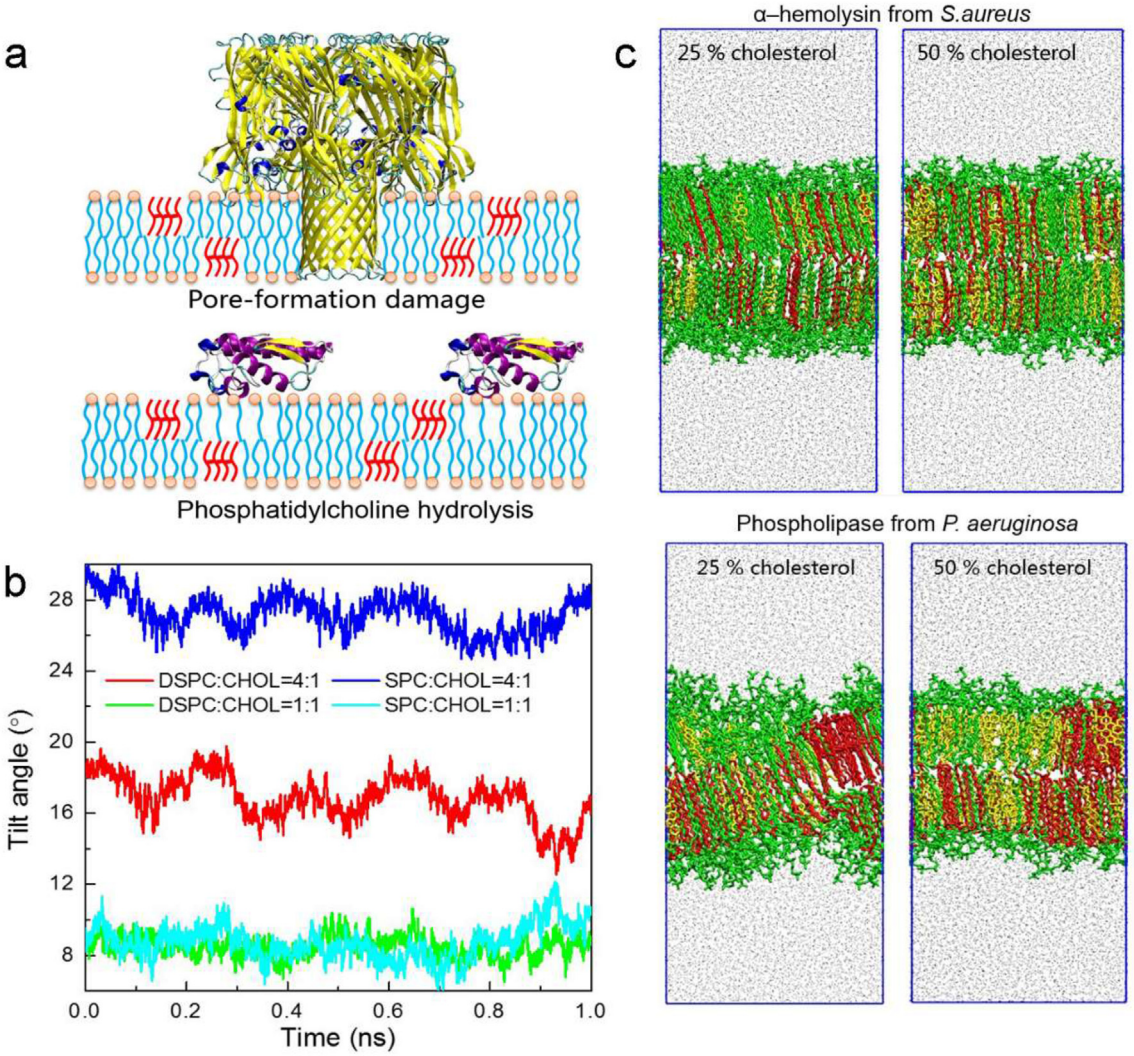

Fig. 5. Representative simulation snapshots of PDA lipid membrane induced by toxins from *S. aureus* and *P. aeruginosa*. (a) Two representative modes of action between bacterial toxins and bio-membranes. Pore-formation damage and phospholipid hydrolysis of bio-membranes induced by α–hemolysin and phospholipase. The red part in the lipid bilayer was desiccated as conjugated PDA. (b) Response of PDA tilt angle θ to the two bacterial toxins α–hemolysin and phospholipase, for the PDA-lipid membrane system. SPC designated as hydrolyzed DSPC by phospholipase; CHOL: cholesterol; DSPC: 1,2-distearoyl-*sn*-glycero-3-phosphocholine18:0; (c) simulation snapshots induced by α–hemolysin (upper figures) and phospholipase (lower figures) for the PDA-lipid complexes composed of 25 % and 50 % cholesterol, respectively. PDA (red), DSPC/SPC (green), CHOL (yellow).

each bacterial strain for multiple tests (≥20) were tabulated in Fig. 4b. The histogram of the R value for each bacteria was based on the average of 20 tested R values. Each PDA-lipid array comprised different concentrations of cholesterol (Table S1). The results of different PDA-lipid arrays for each bacterial strain showed significant differences ($P < 0.05$). Therefore, each PDA-lipid array corresponding to different color patterns provided a piece of convincing evidence for the feasibility of bacterial 'fingerprint' recognition.

3.4. MD analysis

The elaborate interplay of intermolecular interactions among bacterial toxins, and lipid membranes including cholesterol concentration and PDAs should play important roles in PDA-lipid sensitivity. To unravel the intrinsic mechanism of the striking different responses of bacterial toxins to PDA-lipid complexes comprising various contents of cholesterol, a theoretical protocol combining large-scale molecular dynamics (MD) simulations was adopted in the study. α–hemolysin from *S. aureus* and phospholipase from *P. aeruginosa* as model bacterial toxins, 20 % and 50 % cholesterol were chosen to be embedded within PDA-lipid moieties as two amphiphilic models in the study. The setup of the PDA-lipid bilayer system used in the simulation is fully described in the experimental section. The MD analysis was used to validate that the insertion of cholesterol may influence PDA sensitivity to bacterial toxins. The possible modes of action of these two selected toxins are illustrated in Fig. 5a. Interactions occurring at lipid bilayers either by lipid degradation via phospholipase or pore-forming damage via α–hemolysin may alter tilt angles of the PDA backbone, causing subsequent colorimetric responses. Representative snapshots of the equilibrated PDA-lipid bilayers comprising 25 % and 50 % cholesterol upon perturbation of the two toxins are shown in Fig. 5c. PDA-lipid bilayers comprising 25 % cholesterol showed noticeable structural features that PDA tails were significantly tilted from the bilayer's normal direction. The more pronounced tilted angle caused by phospholipase compared to that of α-hemolysin indicated the greater transformation of the PDA backbone thus resulting in more intense color conversion. Whereas lipid bilayers comprising 50 % cholesterol exhibited a little tilted angle of PDA by both toxins, causing less intense of chromatic color conversion. The MD results were consistent with the experimental results and due to the large computational workload, we only selected two PDA models and two types of

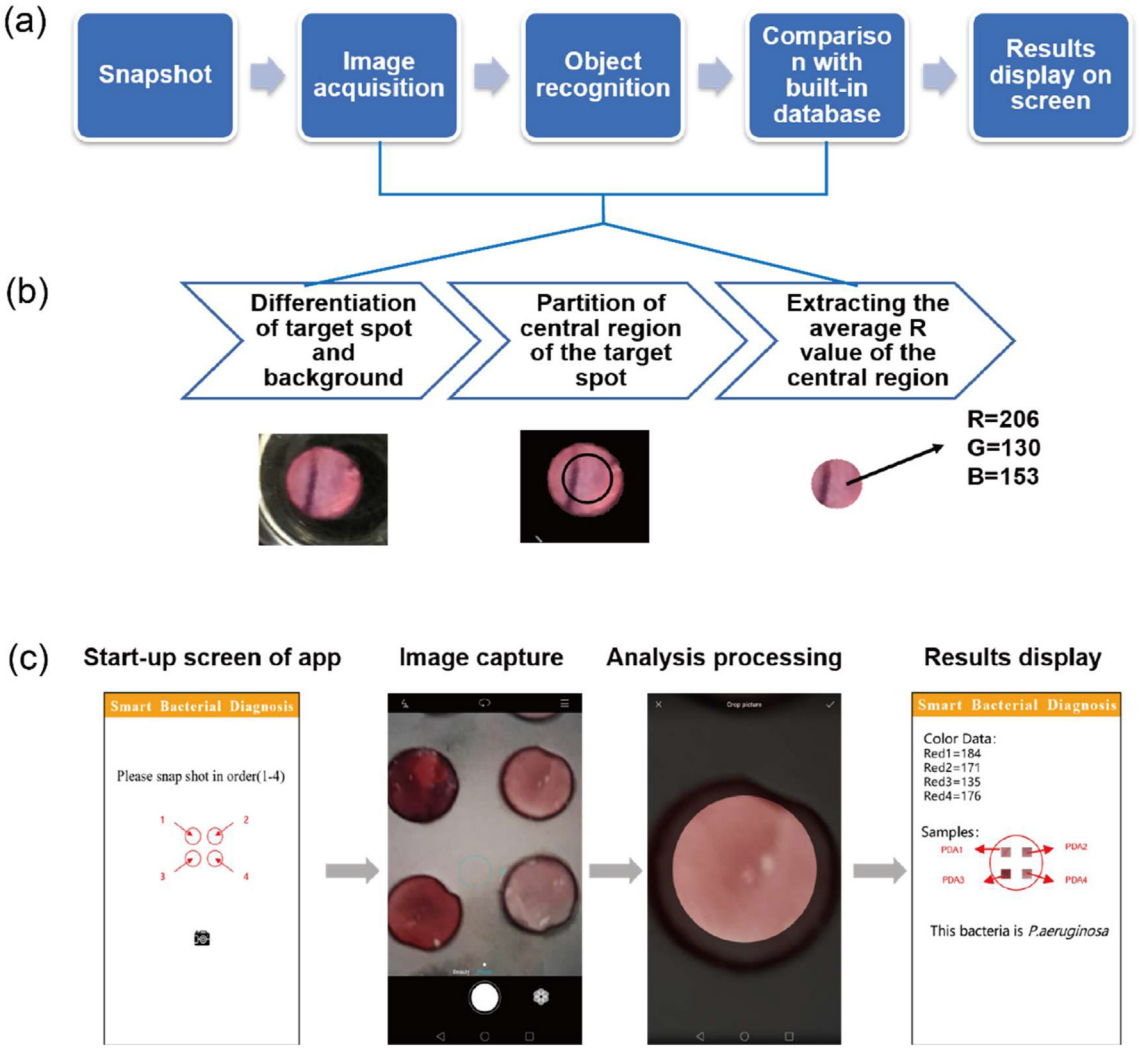

Fig. 6. Smartphone-based bacteria sensing procedure. (a) Description of the procedure of smartphone-based sensing platform; (b) specific processing details of the target image; (c) panels of smartphone screenshot indicates start-up screen, image capture from 1-2-3-4 in order, analysis processing and results display screen.

representative toxins for MD analysis.

3.5. Smartphone-based PDA arrayed membrane chip for bacteria identification

The membrane-based PDA array enabled visual distinction among 5 bacterial strains, whereas the differences in color finger patterns were quite small, and with the increased numbers of bacterial detection, the identification process by visualization would be exceptionally challenging. To facilitate users' understanding and operation, a smartphone-based platform was integrated with PDA arrays for a convenient, user-friendly POCT device to provide detection sensitivity and the subsequent antimicrobial sensitivity equivalent to that of the clinical testing. To quantify the changes caused by bacteria in PDA arrays, R values corresponding to each bacteria were analyzed by Image J software. Deeper red colors corresponded to higher R values. The database of R value arrays corresponding to each bacterium was uploaded to a Bacterial Diagnosis app which was developed by using an Android Studio app. A camera button and four small circles for guiding the positions of the four components of PDA spots were included in the start-up interface (Fig. 6c). The four PDA spots were aligned with the four circles and snapshots were taken in sequence (Fig. 6c). The developed app then extracted the R values of each corresponding circular region and started to calculate and compare the R values of each PDA array with the built-in R database for specific bacteria identification (Fig. 4b). The unknown bacteria was identified, which was displayed on the smartphone screen (Fig. 6c). To limit image analysis errors caused by ambient light and weather, as well as performance differences of built-in cameras, the R values were normalized by using calibration factors corresponding to RGB values which were obtained from spots with a white background among the four PDA spots, as shown in Fig. 6b. The normalized R value of the four PDA spots corresponding to each bacteria was displayed on the screen and compared to the preloaded database. The matching result was displayed on the screen, achieving bacterial identification based on a smartphone, as indicated in Fig. 6c (results display). In the PDA membrane-based POCT scenario, the bacteria in urine can be identified in $\sim$ 1 h, when applied to UTI diagnosis. Therefore, the prescription can be only treated for the patients who have been bacteria infected rather than treating all the patients with suspected clinical symptoms of UTI. In addition, by utilizing such a sensing protocol, the accuracy of identification was evaluated for the three chosen bacterial strains, with an accuracy of 93 %, 93 %, and 83 % in *P. aeruginosa*, *S. aureus,* and *E. coli* ($n \geq 30$), respectively. Based on these observations, we conclude that PDA arrayed membrane chip can be an effective POCT in resource-limited regions, not only for rapid detection of suspected bacterial strains but also to provide suggestions for drug administration to prevent undesirable side effects of drug resistance.

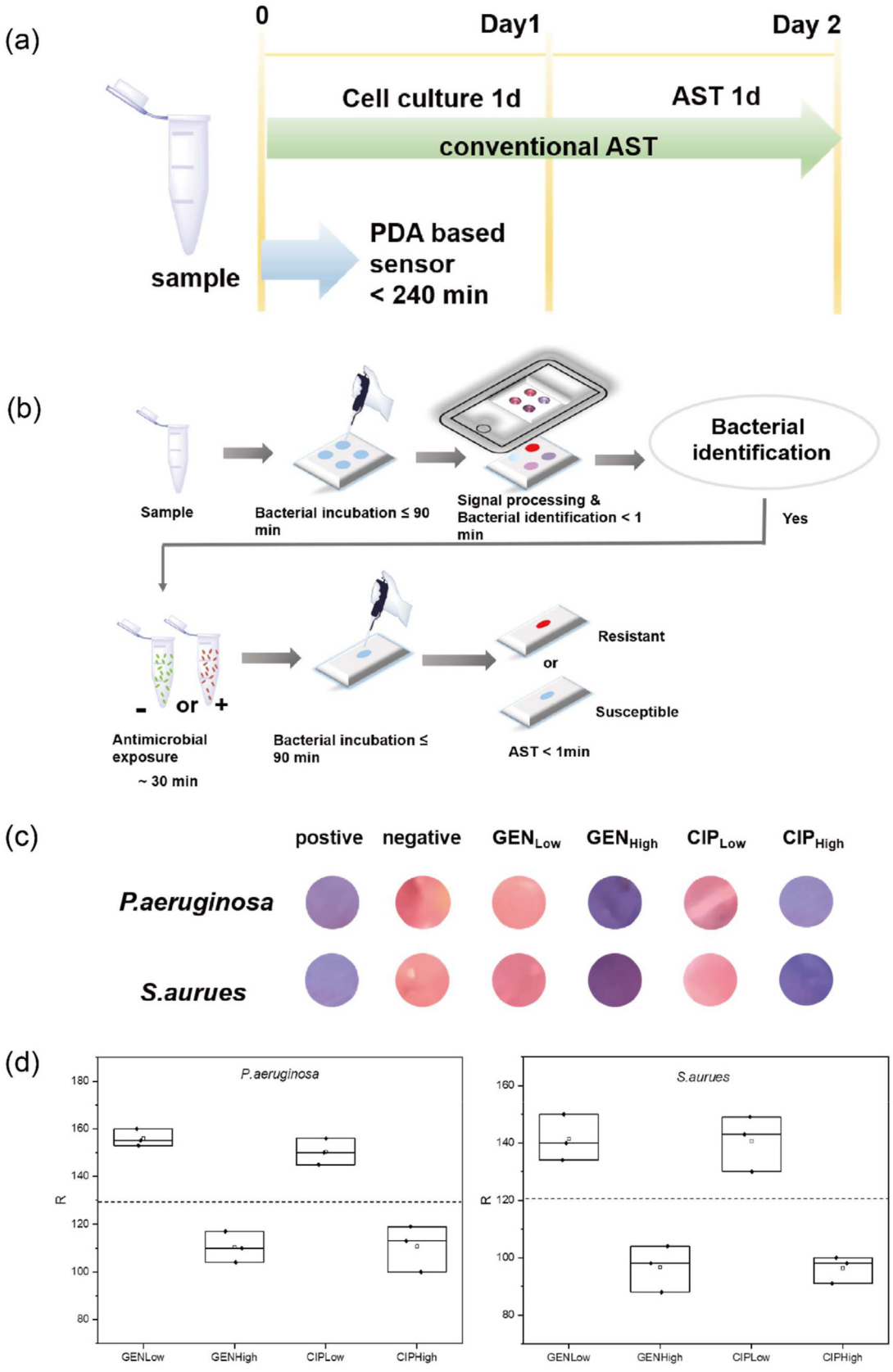

Fig. 7. Antimicrobial susceptibility test (AST) of PDA membrane chip. (a) A conventional AST takes longer than a PDA membrane chip which tests drug resistance in less than 4 h. (b) Schematic illustration of the procedure of AST test by PDA membrane chip. (c) Chromatic results of AST performed by PDA membrane chip for two bacterial strains, *P. aeruginosa* and *S. aureus.* Two antimicrobials including gentamicin sulfate and ciprofloxacin were tested in two dosages according to MIC results. (d) Quantification of red color intensity measurements of the two bacteria strains for testing resistant and susceptible cases. The experiment was carried out in triplicate.

3.6. PDA based AST

Conventional AST (antimicrobial susceptibility test) requires laboratory manipulation based on bacterial culturing and colony counting. AST normally takes at least 2 days for bacterial identification, which is unrealistic and time-consuming in point-of-care applications [68] (Fig. 7a). Quick AST results based on point-of-care can assist carers in identifying the right antimicrobials among a few recommended drugs, reducing further complications of drug resistance at the level of primary care [69, 70]. As *P. aeruginosa* and *S. aureus* are the most common pathogens that cause hospital acquired infections, we focused on these species for the study of AST. On confirming that the pathogen was *S. aureus* and *P. aeruginosa* by the PDA-based membrane chip, a rapid PDA membrane chip-based AST can be performed as indicated in Fig. 7b.

The color intensity of bacteria exposed to different concentrations of antimicrobials was shown and compared. Therefore, susceptible and resistant bacterial strains can be categorically identified within 4 h (Fig. 7b). In the present study, if the measured viable bacterial cells were significantly reduced reflected by decreased red intensity observed by naked eyes, it indicated that the bacteria were sensitive to the antimicrobials. As a proof of concept, the two bacterial strains were treated with two broad-spectrum antimicrobials, gentamicin sulfate and ciprofloxacin at minimum inhibitory concentrations (MIC) represented as $GEN^{low/high}$ and $CIP^{low/high}$ for each bacteria to identify drug-resistant or susceptible bacteria. MIC_{50} and MIC_{90} of gentamicin and ciprofloxacin were measured (Table S2) and designated as GEN^{low}/CIP^{low} and GEN^{low}/CIP^{high}, respectively. For *P. aeruginosa*, 50 μg/mL and 200 μg/mL were represented as GEN^{low} and GEN^{high}, whereas 10 μg/mL and 100 μg/mL as CIP^{low} and CIP^{high}, respectively; for *S. aureus*, 40 μg/mL and 300 μg/mL were as GEN^{low} and GEN^{high}, 32 μg/mL and 500 μg/mL as CIP^{low} and CIP^{high}. After confirming the identity of bacteria by PDA arrayed membrane chip, one PDA-lipid spot which can cause the most noticeable colorimetric transition was chosen for subsequent AST of confirmed bacteria. Here, for instance, Ves 1, causing the highest R intensity in both *S. aureus* and *P. aeruginosa*, was used for the AST study. Fig. 7c shows both negative and positive results of the performance of the PDA membrane chip, with negative and positive controls. The positive controls (susceptible ones) in both *P. aeruginosa* and *S. aureus* showed a visual dark blue signal, suggesting a significant reduction in the number of viable bacteria and thus causing no colorimetric transition of PDA spot, whereas the negative controls (resistant ones) showed visual purple/red signal, indicating that there were no significant changes in the number of viable bacterial cells.

The red color intensity corresponding to the distinguishable color differences by the naked eye was summarized and analyzed, shown in Fig. 7c–e. The appropriate concentration of a specific antimicrobial can be quickly determined by using the PDA-based method. Although AST remains a gold-standard method for evaluating drug susceptibility, the PDA-based colorimetric sensor can provide a fast (within 4 h) and simple method to identify the drug susceptibility for common infectious cases such as UTI at point-of-care. Based on such a method, we can quickly determine the right concentration of specific antimicrobials. In the present study, we mainly focused on identifying the appropriate antimicrobials from the empirical ones to fight infection, which is of vital interest to patients in point-of-care settings.

4. Conclusion

We have developed a highly simple and accurate bacteria sensing platform that can be operated by a conventional smartphone. The platform was based on immobilizing an array of four PDA-lipid complexes on a paper-like PVDF membrane. A database of colorimetric transition in terms of R intensity was constructed on the basis of chromatic responses of four PDA-lipid complexes to five bacterial species. Chromatic color transitions occurred upon exposure of the PDA-lipid array to unknown bacteria, which was imaged by a built-in smartphone camera and processed by the app. The colorimetric transition was compared with the database promoted by 5 bacterial species, enabling the smartphone app to identify the unknown bacteria. Each bacteria exhibited a unique color 'fingerprint' pattern on the PDA arrayed membrane chip due to different mechanisms of bacterial toxins with biomembrane-like lipids composed of different contents of cholesterol. Therefore, the development of a smartphone app is to supplement the shortcomings caused by visual identification such as insufficient sensitivity, although the relatively high concentration of bacteria can be visually distinguished by using only a PDA-based membrane chip. The viable bacterial cells can be determined as low as 10^4 CFU/mL with high accuracy, with the aid of a smartphone app.

Furthermore, a rapid AST by PDA-based membrane chip was examined to identify the bacterial susceptibility to the two broad-spectrum antimicrobials within 4 h. The rapid AST provides an early screening of antimicrobial prescription and provides appropriate prescribed concentrations of drugs, which can further avoid the occurrence of drug resistance. The study on the AST test is only a preliminary attempt. Further improvement needs to evaluate the quantitative relationship between color intensity and bacterial concentration, to establish a quantitative detection sensor for bacteria.

Overall, the proposed bacteria sensing platform based on PDA-lipid complexes is an ideal POCT device with minimal training and no additional electricity requirement, which may offer an extremely convenient and simple way for bacterial infection diagnostics, especially in resource-limited settings.

Declaration of statement

The submission of this article has not been published previously and it is not under consideration for publication elsewhere. The submission of the article is approved by all authors. If accepted, it will not be published elsewhere in the same form, in English or in any other language, including electronically without the written consent of the copyright-holder.

CRediT authorship contribution statement

Yue Zhou: Writing – original draft. **Yumeng Xue:** Writing – original draft. **Xubo Lin:** Methodology, Validation. **Menglong Duan:** Methodology, Validation. **Weili Hong:** Validation. **Lina Geng:** Validation. **Jin Zhou:** Conceptualization, Funding acquisition, Writing – review & editing, Supervision. **Yubo Fan:** Funding acquisition, Supervision.

Declaration of competing interest

The authors declare that they have no known competing financial interests or personal relationships that could have appeared to influence the work reported in this paper.

Acknowledgments

This study was supported by National Natural Science Foundation of China grant (Nos. T2288101, U20A20390, 11827803,12332019).

Appendix A. Supplementary data

Supplementary data to this article can be found online at https://doi.org/10.1016/j.smaim.2023.10.002.

References

[1] M.N. Toosky, J.T. Grunwald, D. Pala, B. Shen, W.A. Zhao, C. D'Agostini, F. Coghe, G. Angioni, G. Motolese, T.J. Abram, E. Nicolai, A rapid, point-of-care antibiotic susceptibility test for urinary tract infections, J. Med. Microbiol. 69 (1) (2020) 52–62.

[2] P. Yager, G.J. Domingo, J. Gerdes, Point-of-care diagnostics for global health, Annu. Rev. Biomed. Eng. 10 (2008) 107–144.
[3] I.J. Michael, T.-H. Kim, V. Sunkara, Y.-K. Cho, Challenges and opportunities of centrifugal microfluidics for extreme point-of-care testing, Micromachines 7 (2) (2016).
[4] J. Craig, I. Frost, A. Sriram, J. Nuttall, G. Kapoor, Y. Alimi, J.K. Varma, Development of the first edition of African treatment guidelines for common bacterial infections and syndromes, J. Publ. Health Afr. 12 (2) (2021).
[5] K. Malmros, B.D. Huttner, C. McNulty, J. Rodriguez-Bano, C. Pulcini, T. Tangden, F. Thalhammer, N. Delvaux, S. Heytens, L. Bjerrum, M. Wuorela, F. Caron, F. Wagenlehner, J.M. Prins, J.B. Haug, R. Kozlov, A. Barac, B. Beovic, M. de Cueto, E.U.W. Grp, Comparison of antibiotic treatment guidelines for urinary tract infections in 15 European countries: results of an online survey, Int. J. Antimicrob. Agents 54 (4) (2019) 478–486.
[6] A. Eroglu, E.A. Alasehir, Evaluation of treatment applications and antibiotic resistance rates for community acquired urinary tract infections in Turkey and a review of the literature, J. Urol. Surg. 7 (2) (2020) 114–119.
[7] B. Mishra, S. Srivastava, K. Singh, A. Pandey, J. Agarwal, Symptom-based diagnosis of urinary tract infection in women: are we over-prescribing antibiotics? Int. J. Clin. Pract. 66 (5) (2012) 493–498.
[8] M.L. Wilson, L. Gaido, Laboratory diagnosis of urinary tract infections in adult patients, Clin. Infect. Dis. 38 (8) (2004) 1150–1158.
[9] C.E. George, G. Norman, G.V. Ramana, D. Mukherjee, T. Rao, Treatment of uncomplicated symptomatic urinary tract infections: resistance patterns and misuse of antibiotics, J. Fam. Med. Prim. Care 4 (3) (2015) 416–421.
[10] A. Manz, N. Graber, H.M. Widmer, Miniaturized total chemical analysis systems: a novel concept for chemical sensing, Sensor. Actuator. B Chem. 1 (1) (1990) 244–248.
[11] A.J. deMello, Control and detection of chemical reactions in microfluidic systems, Nature 442 (7101) (2006) 394–402.
[12] G.M. Whitesides, The origins and the future of microfluidics, Nature 442 (7101) (2006) 368–373.
[13] M.G. Mauk, Calling in the test: smartphone-based urinary sepsis diagnostics, EBioMedicine 37 (2018) 11–12.
[14] T. Laksanasopin, T.W. Guo, S. Nayak, A.A. Sridhara, S. Xie, O.O. Olowookere, P. Cadinu, F.X. Meng, N.H. Chee, J. Kim, C.D. Chin, E. Munyazesa, P. Mugwaneza, A.J. Rai, V. Mugisha, A.R. Castro, D. Steinmiller, V. Linder, J.E. Justman, S. Nsanzimana, S.K. Sia, A smartphone dongle for diagnosis of infectious diseases at the point of care, Sci. Transl. Med. 7 (273) (2015).
[15] A. Nougairede, L. Ninove, C. Zandotti, X. de Lamballerie, C. Gazin, M. Drancourt, B. La Scola, D. Raoult, R.N. Charrel, Point of care strategy for rapid diagnosis of novel A/H1N1 influenza virus, PLoS One 5 (2) (2010).
[16] K. Guk, J.O. Keem, S.G. Hwang, H. Kim, T. Kang, E.K. Lim, J. Jung, A facile, rapid and sensitive detection of MRSA using a CRISPR-mediated DNA FISH method, antibody-like dCas9/sgRNA complex, Biosens. Bioelectron. 95 (2017) 67–71.
[17] E.K. Lim, K. Guk, H. Kim, B.H. Chung, J. Jung, Simple, rapid detection of influenza A (H1N1) viruses using a highly sensitive peptide-based molecular beacon, Chem. Commun. 52 (1) (2016) 175–178.
[18] J. Moon, J. Byun, H. Kim, E.K. Lim, J. Jeong, J. Jung, T. Kang, On-site detection of aflatoxin B1 in grains by a palm-sized surface plasmon resonance sensor, Sensors 18 (2) (2018).
[19] W. Zhao, M.A. Brook, Y.F. Li, Design of gold nanoparticle-based colorimetric biosensing assays, Chembiochem 9 (15) (2008) 2363–2371.
[20] T.T. Le, P.X. Chang, D.J. Benton, J.W. McCauley, M. Iqbal, A.E.G. Cass, Dual recognition element lateral flow assay toward multiplex strain specific influenza virus detection, Anal. Chem. 89 (12) (2017) 6781–6786.
[21] N. Wiriyachaiporn, H. Sirikett, W. Maneeprakorn, T. Dharakul, Carbon nanotag based visual detection of influenza A virus by a lateral flow immunoassay, Microchim. Acta 184 (6) (2017) 1827–1835.
[22] C.Y. Lin, Y.J. Guo, M.M. Zhao, M. Sun, F. Luo, L.H. Guo, B. Qiu, Z.Y. Lin, G.N. Chen, Highly sensitive colorimetric immunosensor for influenza virus H5N1 based on enzyme-encapsulated liposome, Anal. Chim. Acta 963 (2017) 112–118.
[23] T.T. Le, B. Adamiak, D.J. Benton, C.J. Johnson, S. Sharma, R. Fenton, J.W. McCauley, M. Iqbal, A.E.G. Cass, Aptamer-based biosensors for the rapid visual detection of flu viruses, Chem. Commun. 50 (98) (2014) 15533–15536.
[24] S. Seo, J. Lee, E.J. Choi, E.J. Kim, J.Y. Song, J. Kim, Polydiacetylene liposome microarray toward influenza A virus detection: effect of target size on turn-on signaling, Macromol. Rapid Commun. 34 (9) (2013) 743–748.
[25] A. Reichert, J.O. Nagy, W. Spevak, D. Charych, Polydiacetylene liposomes functionalized with sialic-acid bind and colorimetrically detect influenza-virus, J. Am. Chem. Soc. 117 (2) (1995) 829–830.
[26] S.G. Hwang, K. Ha, K. Guk, D.K. Lee, G. Eom, S. Song, T. Kang, H. Park, J. Jung, E.-K. Lim, Rapid and simple detection of Tamiflu-resistant influenza virus: development of oseltamivir derivative-based lateral flow biosensor for point-of-care (POC) diagnostics, Sci. Rep. 8 (1) (2018) 12999.
[27] Y.K. Jung, T.W. Kim, J. Kim, J.M. Kim, H.G. Park, Universal colorimetric detection of nucleic acids based on polydiacetylene (PDA) liposomes, Adv. Funct. Mater. 18 (5) (2008) 701–708.
[28] Y.K. Jung, H.G. Park, J.M. Kim, Polydiacelylene (PDA)-based colorimetric detection of biotin-streptavidin interactions, Biosens. Bioelectron. 21 (8) (2006) 1536–1544.
[29] Y.K. Jung, H.G. Park, Colorimetric detection of clinical DNA samples using an intercalator-conjugated polydiacetylene sensor, Biosens. Bioelectron. 72 (2015) 127–132.
[30] D.E. Wang, Y.L. Wang, C. Tian, L.L. Zhang, X. Han, Q. Tu, M.S. Yuan, S. Chen, J.Y. Wang, Polydiacetylene liposome-encapsulated alginate hydrogel beads for Pb2 + detection with enhanced sensitivity, J. Mater. Chem. A 3 (43) (2015) 21690–21698.
[31] E. Cho, S. Jung, Biomolecule-functionalized smart polydiacetylene for biomedical and environmental sensing, Molecules 23 (1) (2018).
[32] D.H. Kang, H.-S. Jung, J. Lee, S. Seo, J. Kim, K. Kim, K.-Y. Suh, Design of polydiacetylene-phospholipid supramolecules for enhanced stability and sensitivity, Langmuir 28 (19) (2012) 7551–7556.
[33] D. Seo, J. Kim, Effect of the molecular size of analytes on polydiacetylene chromism, Adv. Funct. Mater. 20 (9) (2010) 1397–1403.
[34] J. Lee, M. Pyo, S.H. Lee, J. Kim, M. Ra, W.Y. Kim, B.J. Park, C.W. Lee, J.M. Kim, Hydrochromic conjugated polymers for human sweat pore mapping, Nat. Commun. 5 (2014).
[35] J. Lee, S. Seo, J. Kim, Rapid light-driven color transition of novel photoresponsive polydiacetylene molecules, ACS Appl. Mater. Interfaces 10 (4) (2018) 3164–3169.
[36] E. Lebegue, C. Farre, C. Jose, J. Saulnier, F. Lagarde, Y. Chevalier, C. Chaix, N. Jaffrezic-Renault, Responsive polydiacetylene vesicles for biosensing microorganisms, Sensors 18 (2) (2018).
[37] M.C. Lim, Y.J. Shin, T.J. Jeon, H.Y. Kim, Y.R. Kim, Microbead-assisted PDA sensor for the detection of genetically modified organisms, Anal. Bioanal. Chem. 400 (3) (2011) 777–785.
[38] A. Pevzner, S. Kolusheva, Z. Orynbayeva, R. Jelinek, Giant chromatic lipid/polydiacetylene vesicles for detection and visualization of membrane interactions, Adv. Funct. Mater. 18 (2) (2008) 242–247.
[39] T. Eaidkong, R. Mungkarndee, C. Phollookin, G. Tumcharern, M. Sukwattanasinitt, S. Wacharasindhu, Polydiacetylene paper-based colorimetric sensor array for vapor phase detection and identification of volatile organic compounds, J. Mater. Chem. 22 (13) (2012) 5970–5977.
[40] H. Jeon, J. Lee, M.H. Kim, J. Yoon, Polydiacetylene-based electrospun fibers for detection of HCl gas, Macromol. Rapid Commun. 33 (11) (2012) 972–976.
[41] J. Lee, S. Seo, J. Kim, Colorimetric detection of warfare gases by polydiacetylenes toward equipment-free detection, Adv. Funct. Mater. 22 (8) (2012) 1632–1638.
[42] X.N. Wang, X.L. Sun, P.A. Hu, J. Zhang, L.F. Wang, W. Feng, S.B. Lei, B. Yang, W.W. Cao, Colorimetric sensor based on self-assembled polydiacetylene/graphene-stacked composite film for vapor-phase volatile organic compounds, Adv. Funct. Mater. 23 (48) (2013) 6044–6050.
[43] S. Seo, J. Lee, M.S. Kwon, D. Seo, J. Kim, Stimuli-responsive matrix-assisted colorimetric water indicator of polydiacetylene nanofibers, ACS Appl. Mater. Interfaces 7 (36) (2015) 20342–20348.
[44] S. Seo, M.S. Kwon, A.W. Phillips, D. Seo, J. Kim, Highly sensitive turn-on biosensors by regulating fluorescent dye assembly on liposome surfaces, Chem. Commun. 51 (50) (2015) 10229–10232.
[45] J. Zhou, M. Duan, D. Huang, H. Shao, Y. Zhou, Y. Fan, Label-free visible colorimetric biosensor for detection of multiple pathogenic bacteria based on engineered polydiacetylene liposomes, J. Colloid Interface Sci. 606 (2022) 1684–1694.
[46] C.S. Wood, M.R. Thomas, J. Budd, T.P. Mashamba-Thompson, K. Herbst, D. Pillay, R.W. Peeling, A.M. Johnson, R.A. McKendry, M.M. Stevens, Taking connected mobile-health diagnostics of infectious diseases to the field, Nature 566 (7745) (2019) 467–474.
[47] F. Jannah, J.-M. Kim, pH-sensitive colorimetric polydiacetylene vesicles for urease sensing, Dyes Pigments 169 (2019) 15–21.
[48] D. Kim, Y. Cao, D. Mariappan, M.S. Bono Jr., A.J. Hart, B. Marelli, A microneedle technology for sampling and sensing bacteria in the food supply chain, Adv. Funct. Mater. 31 (1) (2021).
[49] M.O. Kim, M.Q. Khan, A. Ullah, P. Duy-Nam, C. Zhu, J.-S. Lee, I.S. Kim, Fabrication and characterization of colorimetric polymer based novel nanofibers for sensing and blocking of bacterial, Mater. Res. Express 7 (8) (2020).
[50] J. Tao, X. Xu, S. Wang, T. Kang, C. Guo, X. Liu, H. Cheng, Y. Liu, X. Jiang, J. Mao, M. Gou, Polydiacetylene-nanoparticle-functionalized microgels for topical bacterial infection treatment, ACS Macro Lett. 8 (5) (2019) 563–568.
[51] P. Vidal, M. Martinez, C. Hernandez, A.R. Adhikari, Y. Mao, L. Materon, K. Lozano, Development of chromatic biosensor for quick bacterial detection based on polyvinyl butyrate-polydiacetylene nonwoven fiber composites, Eur. Polym. J. 121 (2019).
[52] Y. Zhang, P.L. Dawson, T.W. Hanks, J.K. Northcutt, T.-R. Tzeng, W.T. Pennington, Detecting and correlating bacterial populations to visual color change of polydiacetylene-coated filters, Talanta 221 (2021).
[53] M.J. Abraham, T. Murtola, R. Schulz, S. Páll, J.C. Smith, B. Hess, E. Lindahl, GROMACS: high performance molecular simulations through multi-level parallelism from laptops to supercomputers, SoftwareX 1–2 (2015) 19–25.
[54] J.B. Klauda, V. Monje, T. Kim, W. Im, Improving the CHARMM force field for polyunsaturated fatty acid chains, J. Phys. Chem. B 116 (31) (2012) 9424–9431.
[55] J.B. Klauda, R.M. Venable, J.A. Freites, J.W. O'Connor, D.J. Tobias, C. Mondragon-Ramirez, I. Vorobyov, A.D. MacKerell, R.W. Pastor, Update of the CHARMM all-atom additive force field for lipids: validation on six lipid types, J. Phys. Chem. B 114 (23) (2010) 7830–7843.
[56] S. Lee, J. Lee, M. Lee, Y.K. Cho, J. Baek, J. Kim, S. Park, M.H. Kim, R. Chang, J. Yoon, Construction and molecular understanding of an unprecedented, reversibly thermochromic bis-polydiacetylene, Adv. Funct. Mater. 24 (24) (2014) 3699–3705.
[57] U. Essmann, L. Perera, M.L. Berkowitz, T. Darden, H. Lee, L.G. Pedersen, A smooth particle mesh Ewald method, J. Chem. Phys. 103 (19) (1995) 8577–8593.
[58] W.G. Hoover, Canonical dynamics: equilibrium phase-space distributions, Phys. Rev. A 31 (3) (1985) 1695–1697.
[59] S. Nosé, A molecular dynamics method for simulations in the canonical ensemble, Mol. Phys. 52 (2) (1984) 255–268.

[60] M. Parrinello, A. Rahman, Polymorphic transitions in single crystals: a new molecular dynamics method, J. Appl. Phys. 52 (12) (1981) 7182–7190.
[61] B. Hess, H. Bekker, H.J.C. Berendsen, J.G.E.M. Fraaije, LINCS: a linear constraint solver for molecular simulations, J. Comput. Chem. 18 (12) (1997) 1463–1472.
[62] W. Humphrey, A. Dalke, K. Schulten, VMD: visual molecular dynamics, J. Mol. Graph. 14 (1) (1996) 33–38.
[63] X. Wang, Y. Wei, S. Wang, L. Chen, Red-to-blue colorimetric detection of chromium via Cr (III)-citrate chelating based on Tween 20-stabilized gold nanoparticles, Colloids Surf. A Physicochem. Eng. Asp. 472 (2015) 57–62.
[64] X. Sun, T. Chen, S. Huang, L. Li, H. Peng, Chromatic polydiacetylene with novel sensitivity, Chem. Soc. Rev. 39 (11) (2010) 4244–4257.
[65] M.A. Reppy, B.A. Pindzola, Biosensing with polydiacetylene materials: structures, optical properties and applications, Chem. Commun. (42) (2007) 4317–4338.
[66] E. Cho, S. Jung, Biomolecule-functionalized smart polydiacetylene for biomedical and environmental sensing, Molecules 23 (1) (2018) 107.
[67] G.N. Patel, J.D. Witt, Y.P. Khanna, Thermochromism in polydiacetylene solutions, J. Polym. Sci. Polym. Phys. Ed 18 (6) (1980) 1383–1391.
[68] K.M. Kuper, D.M. Boles, J.F. Mohr, A. Wanger, Antimicrobial susceptibility testing: a primer for clinicians, pharmacotherapy, J. Human Pharmacol. Drug Ther. 29 (11) (2009) 1326–1343.
[69] M. Chokshi, B. Patil, R. Khanna, S.B. Neogi, J. Sharma, V.K. Paul, S. Zodpey, Health systems in India, J. Perinatol. 36 (3) (2016) S9–S12.
[70] J. Avesar, D. Rosenfeld, M. Truman-Rosentsvit, T. Ben-Arye, Y. Geffen, M. Bercovici, S. Levenberg, Rapid phenotypic antimicrobial susceptibility testing using nanoliter arrays, Proc. Natl. Acad. Sci. USA 114 (29) (2017) E5787–E5795.